Multidecadal solar radiation trends in the United States and Germany and direct tropospheric aerosol forcing

Beate Liepert
Lamont-Doherty Earth Observatory of Columbia University, Palisades, New York, USA

Ina Tegen
Max Planck Institute for Biogeochemistry, Jena, Germany

Received 23 April 2001; revised 15 October 2001; accepted 1 November 2001; published 26 June 2002.

[1] In recent studies, anthropogenic aerosols have been recognized as important radiative forcing factors of climate because of their ability to scatter and/or absorb sunlight. At clear-sky conditions the direct aerosol forcing at ground is negative and implies less solar heating of the surface because of aerosols. In this study, an intensified direct aerosol forcing of -7 to -8 W/m^2 has been detected in the United States for the interval from 1960 to 1990. In Germany a weakened aerosol forcing of +3 W/m^2 was observed during the same time period. Even though the aerosol forcing is stronger in the eastern United States compared to the western United States, the positive trend is almost equal. We attained these results by scrutinizing clear-sky global solar radiation recordings for these regions and this time period. Additionally, the diurnal cycle and the direct to diffuse ratio of solar radiation were used for constraining the observed trends. Increased absorption and declined light scattering are presumably responsible for the intensified direct aerosol forcing in the United States. While at the same time in Germany, both aerosol absorption and scattering must have declined to explain the parallel weakened aerosol forcing and the increased direct/diffuse ratio. To estimate the possible anthropogenic portion of these observed changes, we compared the observational results with modeled aerosol forcing scenarios retrieved from the Goddard Institute for Space Studies general circulation model (GISS GCM). Modeled surface solar radiation, aerosol optical thickness, and single-scattering albedo are derived from emission trends of anthropogenic sulfate and carbonaceous aerosols. The emission distributions are calculated from fossil fuel consumption databases. On the basis of these simulations we suspect that the declining trend of sulfate burden over Germany between 1960 and 1990 was stronger than estimated with the model. Over the United States the simulated small increase in the carbonaceous aerosol burden was exaggerated in order to explain the observed changes in surface solar radiation, diurnal cycle, and direct/diffuse ratio of surface solar radiation. In addition to emission changes from fossil fuel burning, other reasons explaining the solar radiation trends are also discussed. *INDEX TERMS:* 0345 Atmospheric Composition and Structure: Pollution—urban and regional (0305); 0360 Atmospheric Composition and Structure: Transmission and scattering of radiation; 0368 Atmospheric Composition and Structure: Troposphere—constituent transport and chemistry; 1610 Global Change: Atmosphere (0315, 0325); 3359 Meteorology and Atmospheric Dynamics: Radiative processes; *KEYWORDS:* solar radiation, clear-sky forcing, aerosol, sulfate, carbon, multidecadal

1. Introduction

[2] Early in the global climate change debate, it was recognized that increased fossil fuel usage over the last decades led not only to higher carbon dioxide emissions but also to increased concentrations of particulate matter in the troposphere [e.g., *Hansen and Lacis*, 1990]. Greenhouse gas forcing and its changes over time have been well documented, but aerosol climate forcing and its changes over time remain unclear. Depending on their chemical composition, aerosols can scatter sunlight leading to a net atmospheric cooling, or they can absorb and scatter sunlight leading to a possible net warming or net cooling of the atmosphere, respectively. They also have the ability to affect cloud formation and lifetime, which will not be discussed here. *Kiehl and Briegleb* [1993] speculate that light-scattering anthropogenic sulfate aerosols have the potential to offset greenhouse gas warming in the United States and Germany. *Hansen et al.* [2000] and *Jacobsen* [2001] argue that besides light-scattering sulfate aerosols whose concentrations have successfully been reduced in industrialized

0148-0227/02/2001JD000760$09.00

countries in the last 2 decades, light-absorbing black carbon aerosols played an increasing role in climate change. It is therefore crucial for climate models to correctly describe different aerosol types and their optical properties over time. Most climate models utilize the global climatologies of aerosol optical thickness and single-scattering albedo (a measure of aerosol absorptivity) as optical parameters for direct aerosol forcing calculations. Several authors have published those global climatologies for present-day scenarios [*Schult et al.*, 1997; *Penner et al.*, 1998; *Myhre et al.*, 1998]. In addition to the climatologies of the status quo, *Tegen et al.* [2000] have presented a time-dependent climatology covering the last 50 years. All these climatologies of the various aerosol types (sulfate and carbonaceous aerosol, sea salt, desert dust, and biomass burning aerosol) are based on assumptions derived from energy consumption databases, empirical chemical studies, and tracer transport models. The model-based aerosol climatologies are highly uncertain since only a few direct measurements of aerosol chemical and physical properties exist worldwide to verify the simulated results.

[3] Recently, some integrated field experiments have been performed, and detailed information on aerosol chemistry and radiative forcing has been gathered. For example, the Indian Ocean Experiment (INDOEX), which was an experiment over the tropical northern Indian Ocean revealed unexpected large differences in direct aerosol radiative forcing at the top of the atmosphere (TOA) and the Earth's surface [*Satheesh and Ramanathan*, 2001]. Light-absorbing soot aerosols transported from the south Asian continent were largely responsible for these differences. The Tropospheric Aerosol Radiative Forcing Observation Experiment (TARFOX), the field campaign conducted in the summer of 1996 on the United States eastern seaboard, also demonstrated the unexpected importance of carbonaceous aerosols in the United States east coast haze plume [*Russell et al.*, 1999]. For a site in Germany, similar results with an emphasized black carbon (BC) aerosol forcing at the surface were described by *Keil et al.* [2001]. At this site, aerosol forcings were up to 10 times higher at the surface than at the TOA when polluted air masses were present. These field experiments indicate that changes in direct aerosol forcing due to varying concentrations (optical thickness) and different aerosol types (single-scattering albedo and optical thickness) may be detected more easily on the surface than at the top of the atmosphere. Hence long time trends in surface solar radiation can be directly related to trends in aerosol forcing. Surface solar radiation is also a standard diagnostic variable of general circulation models. On the other hand, analyses of long-term series of surface solar radiation are hampered by the fact that the only data available for a longer time period are broadband pyranometer observations whose aerial coverage is sparse compared to other meteorological parameters.

[4] Nonetheless, this study makes the attempt to scrutinize interdecadal variations of clear-sky global solar radiation recordings for the United States and Germany, which are available for 3 decades. In the second part of this paper we compare our findings with direct aerosol forcing results from climatologies modeled by *Tegen et al.* [2000] that are implemented in the Goddard Institute for Space Studies general circulation model (GISS GCM). The goal of this study is to constrain the temporal trend in aerosol radiative forcing for two selected regions and to investigate the effect of anthropogenic aerosols from fossil fuel burning during this time period for these regions.

2. Observed Surface Solar Radiation Climatologies

[5] The radiation data analyzed in this study stem from the National Solar Radiation Database (NSRDB) of the United States collected and processed by the National Renewable Energy Laboratory (NREL) [*Maxwell et al.*, 1995]. This database (formerly SOLRAD) includes among others hourly solar radiation measurements and hourly cloud cover observations. The solar radiation data are broadband measurements of global radiation and in some cases diffuse radiation. Global radiation is the total energy in a horizontal area, and diffuse radiation refers to the scattered radiative energy from the sky dome in a horizontal area. The instruments measure solar radiation in the wavelength interval from 0.3 to 3.0 μm. We selected 25 records out of 56 for the United States and eight time series for Germany. The selected sites are listed in Table 1. The global radiation data for the United States encompass the years 1961 through 1990, but none of the time series are complete. The diffuse part of the global radiation has been monitored since 1977 and is available through 1990 for 21 sites in the United States (see Table 1). The U.S. data underwent intensive homogeneity tests performed by NREL. For a description of the quality control procedures, see *Maxwell et al.* [1995]. The authors have not performed additional homogeneity tests. *Liepert and Lohmann* [2001] utilized this database for a similar study about the indirect aerosol effect. The study introduced here includes solar radiation time series from the German Radiation Network that have already been analyzed in detail by *Liepert and Kukla* [1997] and *Liepert* [1997]. The German solar radiation records represent western European conditions. The sites in Germany are mainly influenced by local emissions and emissions from the United Kingdom, France, and Benelux. All these countries show a very similar behavior in terms of emission of sulfur dioxide and carbonaceous aerosols. The recordings of global solar radiation began in 1964, and the recordings of diffuse solar radiation began in 1977. For Hamburg and Hohenpeissenberg, diffuse solar radiation records are available from 1964 on. The German measurements were taken with Kipp & Zonen instruments, whereas the U.S. recordings were performed with Eppley pyranometers. This factor should not influence the results of the analyses since each record is self-consistent and we are interested in the relative change over time.

[6] The direct aerosol forcing at the surface is defined as the difference between the solar radiation when aerosols are present and the solar radiation that would reach the ground when aerosols were absent in the otherwise same cloud-free atmosphere. The direct aerosol forcing at the surface is therefore always negative or zero. "Direct" refers to the clear-sky cases when light is directly scattered or absorbed by aerosol particles and clouds are not involved. Since we are mainly interested in the temporal variation of the direct aerosol forcing, the changes over time of the total solar radiation are studied here. An "intensification" of the

Table 1. Global (G) and Diffuse (D) Solar Radiation Observations in the United States and Germany

Station	Latitude, deg	Longitude, deg	Meters Above Sea Level	Observations
Albuquerque, New Mexico	35.03N	106.62W	1619	G and D
Bismarck, North Dakota	46.77N	100.75W	502	G and D
Boise, Idaho	43.57N	116.22W	874	D
Boulder, Colorado	40.00N	105.25W	1625	D
Brownsville, Texas	25.88N	97.42W	6	G
Burns, Oregon	43.57N	119.05W	1271	D
Caribou, Maine	46.87N	68.02W	190	G and D
Columbia, Missouri	38.82N	92.22W	720	G and D
Dodge City, Kansas	37.77N	99.97W	787	G and D
El Paso, Texas	31.78N	106.40W	1194	G and D
Ely, Nevada	39.27N	114.83W	1906	G
Eugene, Oregon	44.12N	123.22W	109	D
Fresno, California	36.77N	119.72W	100	G and D
Great Falls, Montana	47.47N	111.37W	1116	G and D
Lake Charles, Louisiana	30.12N	93.22W	3	G
Lander, Wyoming	42.82N	108.72W	1696	D
Madison, Wisconsin	43.12N	89.32W	262	G and D
Montgomery, Alabama	32.28N	86.40W	62	D
Nashville, Tennessee	36.12N	86.67W	180	G and D
Omaha, Nebraska	41.37N	96.52W	404	G and D
Phoenix, Arizona	33.42N	112.17W	339	G and D
Salt Lake City, Utah	40.77N	111.97W	1288	D
Seattle, Washington	47.45N	122.30W	122	G and D
Sterling, Virginia	38.95N	77.43W	82	G
Tallahassee, Florida	30.37N	84.37W	21	D
Braunlage, Germany	51.72N	10.53E	81	G
Braunschweig, Germany	52.30N	10.45E	601	G and D
Hamburg, Germany	53.63N	10.00E	14	G and D
Hohenpeissenberg, Germany	47.78N	11.02E	975	G and D
Norderney, Germany	53.72N	7.15E	13	G and D
Trier, Germany	49.75N	6.67E	265	G and D
Weihenstephan, Germany	48.40N	11.73E	467	G and D
Würzburg, Germany	49.80N	9.90E	259	G and D

aerosol forcing at the surface would mean a decline in solar radiation, whereas a "weakening" of the aerosol forcing refers to an increase in solar radiation at the surface. The shortwave effect of long-term variations in gas absorption is negligible in the broadband, as are changes in Rayleigh scattering. Only surface albedo changes can interfere because of enhanced multiple reflection between surface and atmosphere. It is assumed that interdecadal albedo changes did not occur.

[7] The clear-sky selection is performed on an hourly basis. On a multidecadal timescale, only visually taken total cloud cover observations are available and are therefore chosen as clear-sky criterion. Clear sky is defined here as zero or one tenth of sky coverage of clouds observed at the beginning and at the end of an hour. It is not clear if this criterion has the tendency to overestimate or to underestimate global solar radiation because of possible cloud contamination [*Liepert*, 1997]. Light reflections on the sides of clouds tend to increase the diffuse and therefore global solar radiation. On the other hand, thin cirrus clouds that shield the Sun may reduce the global radiation. The total effect is site-specific, and we argue that the measurement errors are statistically distributed because of the large number of observations at various different sites. The selection procedure itself can also lead to sampling errors if the sampling is biased toward certain hours where clear sky is more frequent. To avoid this problem, the full diurnal cycle of solar radiation for each station and month (see Figure 1) is calculated. It is averaged over all hourly radiation data of an individual month and an individual hour. It is also necessary to average over the three decadal intervals 1961–1970, 1971–1980, and 1981–1990 since some of the time series unveil major gaps. For example, the 1980s are sparsely covered in the United States, whereas the German records are mostly complete. The resulting bell-shaped radiation data matrices for each decade are the bases for this study. An example of this matrix is shown in Figure 1.

3. Modeled Direct Aerosol Forcing

[8] *Tegen et al.* [2000] developed global aerosol distributions from a global transport model for an external mixture of sulfate and carbonaceous aerosols from fossil fuel burning usage together with other major aerosol types, such as soil dust and sea salt. The aerosol scenarios are described in detail by *Tegen et al.* [2000] and are briefly summarized here.

[9] Changes in aerosol distributions due to changes in emissions of SO_2 and carbonaceous particles from fossil fuel burning are simulated from 1950 through 1990. Emissions of SO_2 are taken from an analysis by *Lefohn et al.* [1999], and the sulfate aerosol distributions were calculated according to *Koch et al.* [1999]. *Lefohn et al.* [1999] used historic statistical data of fossil fuel consumption and metal production. Black carbon (BC) emissions are derived from the United Nations energy statistics database. Emissions of carbonaceous aerosols are highly uncertain. Therefore three

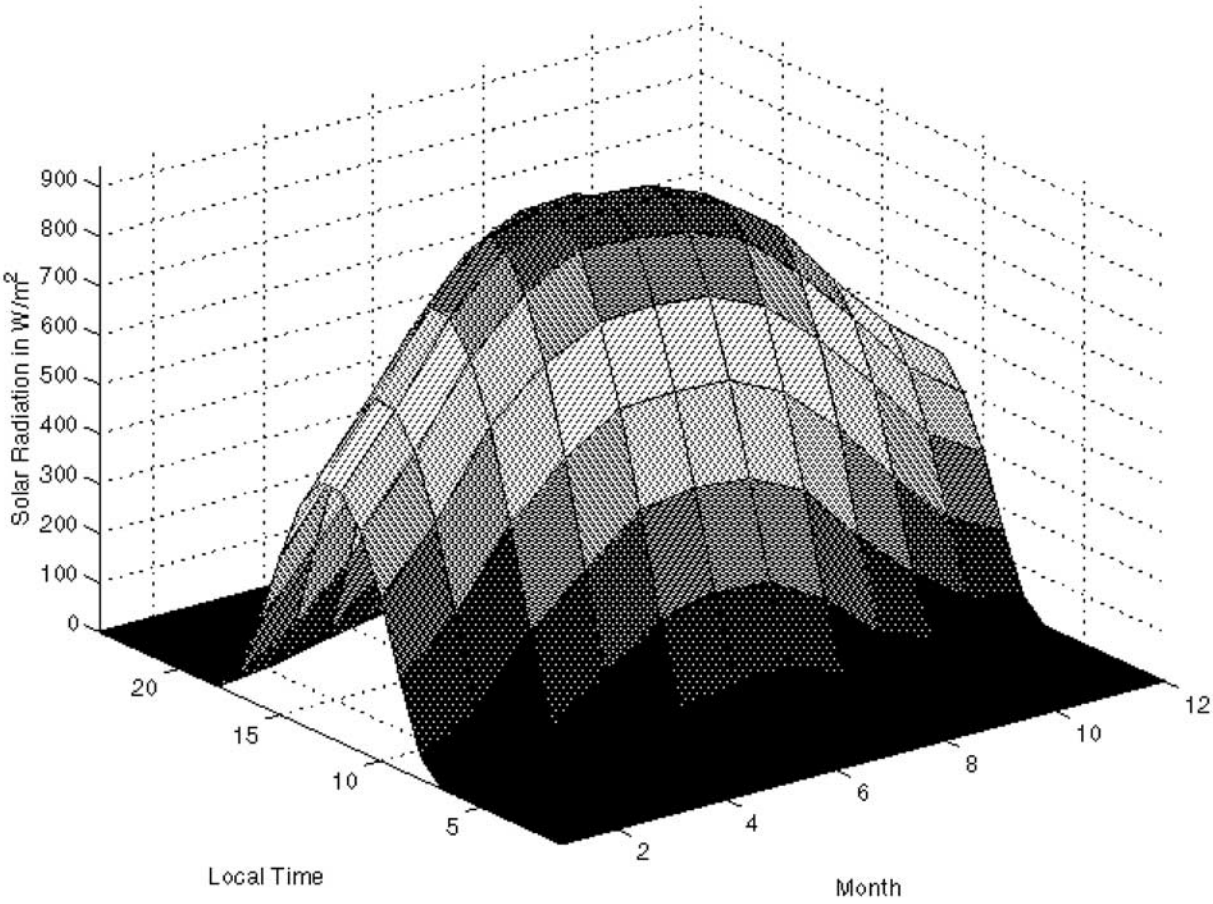

Figure 1. Mean annual and diurnal cycle of global solar radiation at ground for clear skies averaged over the U.S. sites.

scenarios, "high BC," "modest BC," and "low BC," were chosen to cover the uncertainty range of the global emission rates of carbonaceous aerosols. "Modest" denotes BC emissions of 50% of the "high-BC" trend, and "low BC" denotes BC emissions of 20%. Organic carbon (OC) emissions are chosen to be 4 times that of the BC emissions [*Penner et al.*, 1998]. Aerosol size distributions have been kept fixed. The aerosol optical thickness and single-scattering albedo are calculated based on Mie theory. The direct aerosol forcing at the surface is computed for the three scenarios with the radiative transfer model, which is embedded in the GISS GCM [*Tegen et al.*, 2000].

[10] The performance of the sulfate code has been extensively tested [*Koch et al.*, 1999]. Modeled sulfate deposition rates were compared with measured sulfate depositions of the United States and western Europe. For the United States, sulfate depositions from the National Acid Deposition Program/National Trends Network (NADP/NTS) assessment from 1979 to present were used. The sulfate depositions observed by NADP/NTS reflect a decline from 1979 on when the measurements start and a flattening from the middle of the 1980s on. The modeled depositions in the United States are lower than the observed ones at the beginning of the recordings until the early 1980s and agree well afterward [see *Tegen et al.*, 2000, Figure 3]. In Europe the model overestimates sulfate depositions in Germany, while good agreement is achieved in northern Europe. In general, the sulfate concentrations in Europe show a declining trend in both the model and the observations from the late 1970s through 1990 [*Tegen et al.*, 2000].

[11] Although a few measurements of BC and OC concentrations are available in the Northern Hemisphere, no direct long-term measurements of carbonaceous aerosols exist to confirm the modeled changes over time. Alpine ice core data reveal an increasing total carbon trend in the 1960s followed by a decline and flattening of the trend until 1975, which is in agreement with the modeled tendencies [*Lavanchy et al.*, 1999]. The Interagency Monitoring of Protected Visual Environments (IMPROVE) provides aerosol surface concentration data for "rural" stations in the United States [*Malm et al.*, 1994]. The modeled concentrations of carbonaceous aerosol at surface for 1990 showed reasonable agreement with the IMPROVE data [*Tegen et al.*, 2000]. The fine-particle concentrations in the eastern United States IMPROVE sites were higher than in the western part of the country. The west-east gradient is stronger for sulfate than for carbonaceous aerosol. In the western United States the ratio between carbonaceous and sulfate aerosol is 1.8 compared to a ratio of 0.75 in the east (with a ratio between west and east of 0.24 for the sulfate

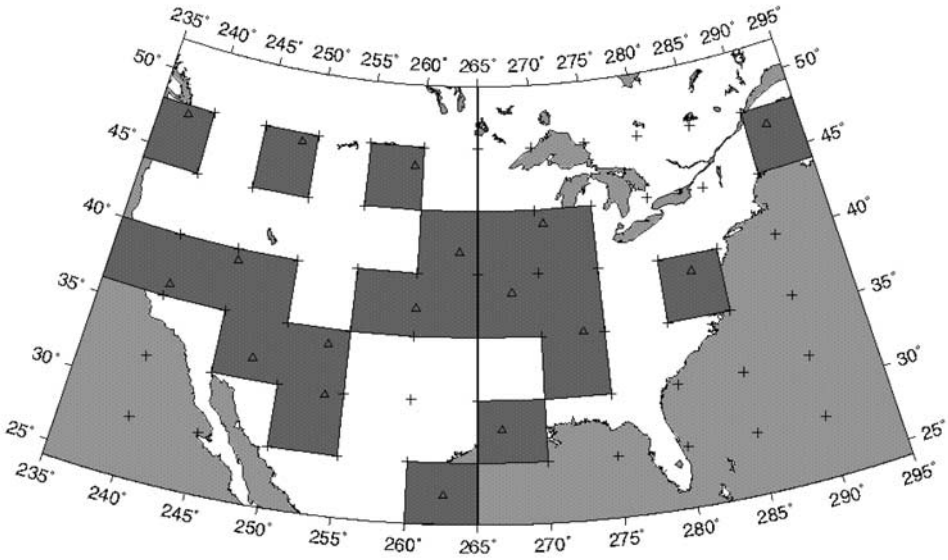

Figure 2. Distribution of the selected global solar radiation grid boxes for the United States. Triangles mark the corresponding observational sites. Demarcation line between western and eastern United States is shown.

concentration and a ratio of 0.55 for carbonaceous aerosol). Similarly, in the model the ratio of carbonaceous to sulfate aerosols is between 1 and 2 in the western United States and is around 0.5–0.8 in the east. This indicates that the aerosol mixture is relatively more absorbing in the western United States.

[12] The direct aerosol forcings derived from aerosol distributions from 1960 to 1990 are computed with the GISS GCM. We employ these results to evaluate the hypothesis that observed changes in direct aerosol forcing are due to aerosol composition variations.

4. Results: Clear-Sky Solar Radiation

4.1. Global Solar Radiation for U.S. Sites

[13] The analysis of clear-sky global solar radiation observations consists of 17 U.S. and eight German time series. The geographical distribution of the U.S. sites and the model grid is shown in Figure 2. The triangles symbolize the observational sites. The corresponding 21 model grid boxes are also included in Figure 2. Some observational sites lie close to the edge of grid boxes, and the averages of two boxes are used. The ''mean solar radiation of the United States'' refers to the average of these 21 boxes or 17 sites. Germany spans over four grid boxes that cover the eight observational sites. The major results of the statistics are summarized in Table 2.

[14] We divide the United States into a western and an eastern part. The demarcation line is 95°W (265° in Figure 2). The seasonal and the diurnal cycles of clear-sky global solar radiation of the west are plotted in Figures 3 and 4 and of the east are plotted in Figures 5 and 6. The western sites received 8 W/m^2 more solar radiation than the eastern sites over the 3 decades (Table 2). The difference in solar radiation between the 1960s and the 1970s is marginal. From the 1970s to the 1980s, however, the solar radiation dropped by 7 W/m^2 in the west and 6 W/m^2 in the east (Figures 3 and 5). This implies an intensification of the direct aerosol forcing at the surface of −7 to −8 W/m^2 or 3% within 3 decades. Note that the 1980s observed average is biased toward the second half of the decade because the recordings have gaps earlier on in the 1980s. If the 1980s were completely covered and a trend existed, the difference would be smaller. The observed difference in clear-sky solar radiation between the western and the eastern part of the United States can be caused by different elevation and latitude or by a strong west-east gradient of aerosol concentrations as observed for the IMPROVE data [*Malm et al.*, 1994].

[15] Following, we compare observational solar radiation with modeled clear-sky solar radiation for the three aerosol

Table 2. Decadal Means of Observed Global Solar Radiation ($G_{observed}$) and Decadal Range of Modeled Global Solar Radiation (G_{model}), Aerosol Optical Thickness (AOT), and Single-Scattering Albedo (SSA) for Three Aerosol Scenarios

	1960s	1970s	1980s
	Western United States		
$G_{observed}$, W/m^2	244	243	236
G_{model}, W/m^2	253–254	253–254	252–253
AOT model	0.11–0.14	0.12–0.16	0.13–0.18
SSA model	0.946–0.923	0.948–0.922	0.947–0.917
	Eastern United States		
$G_{observed}$, W/m^2	236	235	229
G_{model}, W/m^2	230–232	229–231	229–230
AOT model	0.15–0.20	0.17–0.23	0.18–0.26
SSA model	0.952–0.922	0.955–0.922	0.953–0.916
	Germany		
$G_{observed}$, W/m^2	190	190	193
G_{model}, W/m^2	171–178	173–180	177–181
AOT model	0.21–0.45	0.22–0.41	0.20–0.37
SSA model	0.940–0.885	0.948–0.895	0.950–0.898

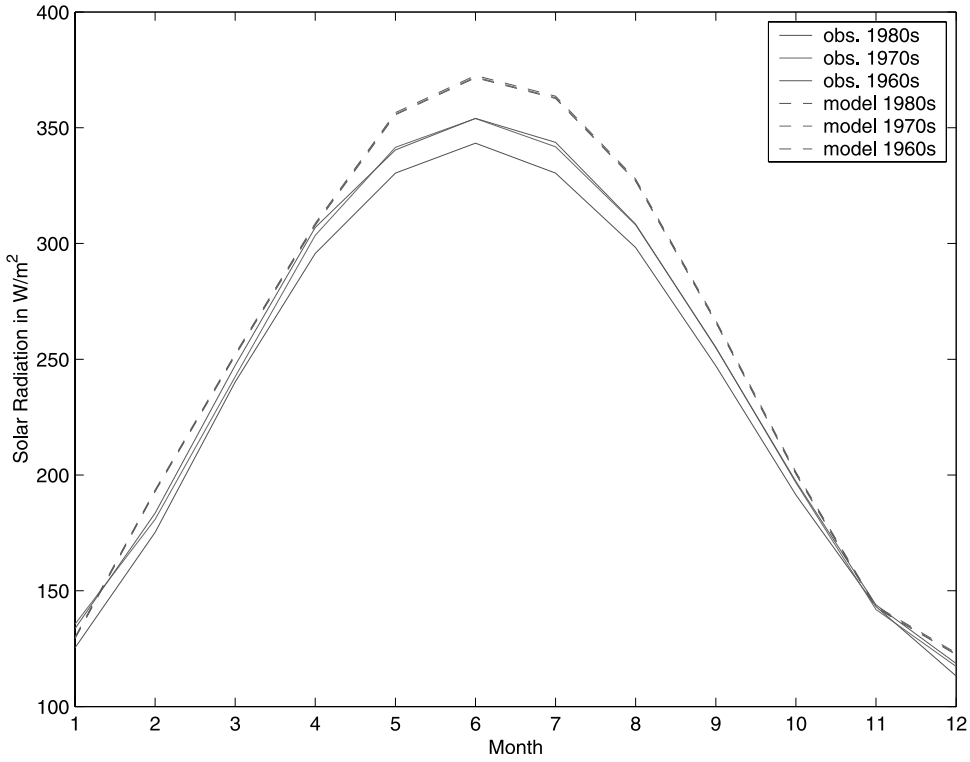

Figure 3. Decadal mean clear-sky global solar radiation at the surface for the western United States. Solid lines are the observations, and dashed lines are the modeled solar radiation monthly means for the high–black carbon (BC) scenario. See color version of this figure at back of this issue.

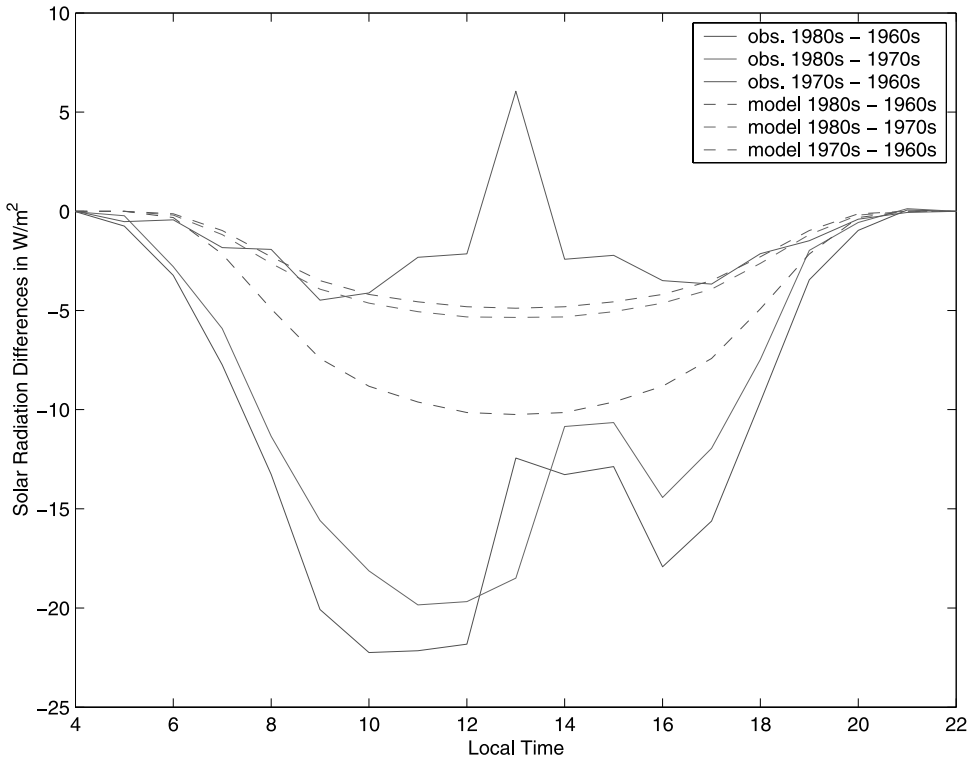

Figure 4. Differences in decadal mean diurnal cycles of clear-sky global solar radiation at the surface for the western United States. Solid lines are the observations, and dashed lines are the modeled differences for the high-BC scenario. See color version of this figure at back of this issue.

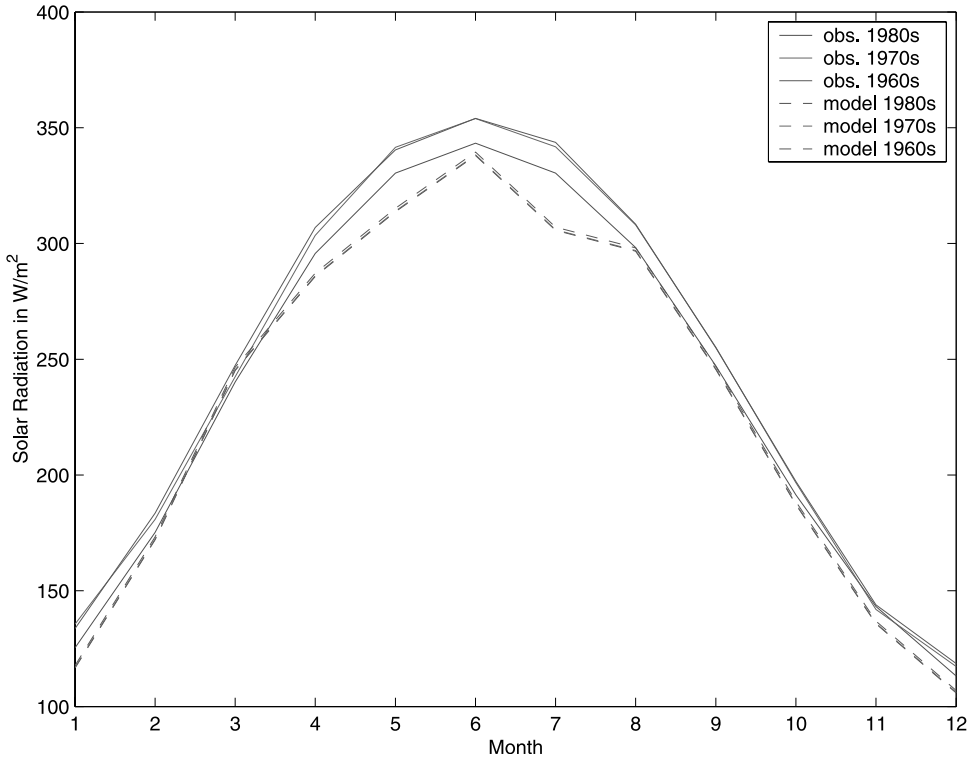

Figure 5. Decadal mean clear-sky global solar radiation at the surface for the eastern United States. Solid lines are the observations, and dashed lines are the modeled solar radiation monthly means for the high-BC scenario. See color version of this figure at back of this issue.

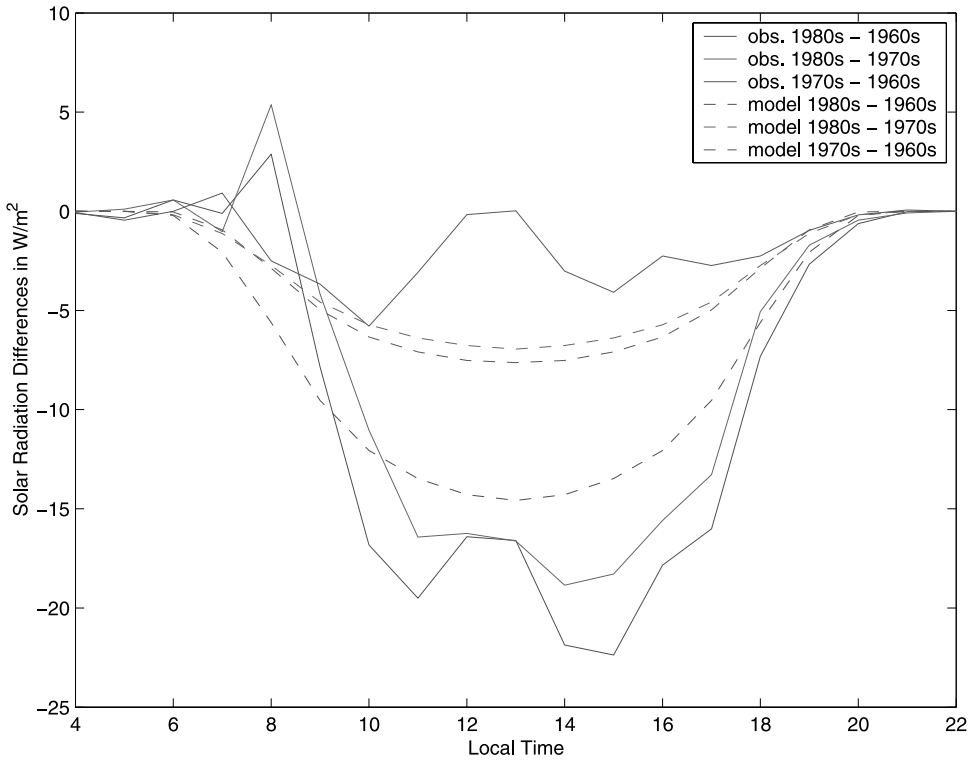

Figure 6. Differences in decadal mean diurnal cycles of clear-sky global solar radiation at the surface for the eastern United States. Solid lines are the observations, and dashed lines are the modeled differences for the high-BC scenario. See color version of this figure at back of this issue.

scenarios to constrain the anthropogenic aerosol effect. The different seasonal cycles of clear-sky global solar radiation monthly means for the three decades 1960s, 1970s, and 1980s are illustrated in Figures 3 and 4.

[16] As shown in Table 2 the modeled surface solar radiation is slightly underestimated (by 2–4 W/m^2) for the eastern part and is overestimated from 10–17 W/m^2 for the western sites of the United States. The 1980s decadal mean solar radiation of the eastern sites is in very good agreement with the observational mean, whereas the modeled solar radiation in the preceding decades is too low when compared to observations. The model does not capture the observed sharp drop of solar radiation from the 1970s to the 1980s in both regions (6 W/m^2 in the west and 7 W/m^2 in the east) even with the maximum aerosol scenario. The modeled intensification of the aerosol forcing is only 1–2 W/m^2. This indicates that an increase in carbonaceous aerosol concentrations by a factor of 4 does not significantly change the average global solar radiation in the United States in the model. It remains unclear to what extent the observed 6–7 W/m^2 decline in clear-sky solar radiation from the1970s to 1980s is caused by measurement errors, by changes in aerosol forcing that were not simulated, or other effects.

4.2. Diurnal Cycles for U.S. Sites

[17] The investigation of the diurnal cycle provides additional information about aerosol absorptivity and scattering. Figure 4 shows the mean diurnal cycles of modeled and observed global solar radiation in the western United States, and Figure 6 shows the mean diurnal cycles of clear-sky global solar radiation at the surface in the eastern United States for the 3 decades. During the first 2 decades the sign of the trend shifts depending on the solar zenith angle. Around noon, clear-sky surface solar radiation unveils an increase, while at morning and evening hours, decreases are shown from the 1960s to the 1970s. This feature is especially pronounced at the western sites (Figure 4). At the eastern sites the solar radiation reveals no trend at noon hours and a slight negative trend elsewhere. Consequently, the global solar radiation of the high BC-scenario shows good agreement in the first and last hours of the cycle but not during midday (red line). This zenith angle-dependent tendency in direct aerosol forcing points to changes in the ratio of aerosol scattering to absorption and not to general changes in aerosol optical thickness. At high solar zenith angles, changes in aerosol absorption are more effective because of the longer optical path [see also *Russell et al.*, 1999]. Aerosol scattering dominates aerosol absorption at lower zenith angles. On the basis of this observation it can be speculated that concentrations of light-scattering sulfate aerosol might have declined, and absorbing aerosol concentrations like soot might have increased from the 1960s to the 1970s. Hence decreasing sulfate and increasing carbonaceous aerosol concentrations may explain the observed midday weakening and morning and evening intensifying of the aerosol forcing.

[18] The modeled high BC-scenario does show an increase in aerosol optical thickness from 0.14 to 0.16 and no significant decline in single-scattering albedo (0.923–0.917) from the 1960s to the 1970s for the western sites (Table 2). This seems not enough to induce the observed shift in diurnal cycle of the direct aerosol forcing (Figure 4). Hence for the 1960s and 1970s the model seems to underestimate the changing ratio of absorbing to scattering aerosols. In the consecutive decade from the 1970s to the 1980s the observed difference in global solar radiation is negative throughout the diurnal cycle (Figure 4, green line). However, even this curve has a local maximum around afternoon that might also be caused by the changing aerosol scattering to absorption ratio. For the eastern sites the modeled aerosol optical thickness is generally higher than for the western sites and shows an increase from 0.20 to 0.26 for the high BC-scenario within 3 decades. The modeled single-scattering albedo is around 0.92 as simulated for the western sites. Generally, anthropogenic aerosol trends as modeled here do not seem to explain the diurnal behavior of solar radiation observations from the 1960s to the 1980s.

4.3. Global Radiation for German Sites

[19] For Germany, the observed decadal mean of the clear-sky global solar radiation is 190 W/m^2 for the 1960s. It is constant throughout the 1970s, as was the case for the United States. During the 1980s the observed global solar radiation increased by 3 W/m^2, which is at odds with the observed drop of 7 W/m^2 in North America. The modeled 1960s decadal mean global solar radiation in Germany lies between 171 and 178 W/m^2, depending on which scenario is used. Even the low-BC scenario underestimates the surface solar radiation for clear skies by 10–12 W/m^2. As illustrated in Figure 7, the underestimation occurs mainly in fall and winter, while good agreement is shown in spring, and even an overestimation is shown in summer. As mentioned in section 3, the emission model overestimates the sulfate deposition in Germany. The variability of carbonaceous aerosols from high-BC to low-BC scenario (one quarter) corresponds to a direct aerosol forcing variability of 4–7 W/m^2 depending on which decade, while the effect for the United States stayed around 1 W/m^2 (see range in Table 2). The modeled +3 W/m^2 weakening of the direct aerosol forcing with the low BC-scenario is exactly the observed increase in solar radiation for the German grid boxes between 1960 and 1990. The modeled optical thickness with the low-BC scenario remains effectively unchanged for 3 decades (see Table 2), whereas the modeled single-scattering albedo increases slightly from 0.94 to 0.95. The comparison indicates that the modeled declining aerosol absorption from 1960s to 1980s is realistic. Note that the opposite was computed for the United States.

4.4. Diurnal Cycles for German Sites

[20] Noteworthy is the similarity between the observed German, western, and eastern United States diurnal cycles in the first 2 decades (Figures 4, 6, and 8). In general, global solar radiation increased at low solar zenith angles, while it declined at high angles. Again, this behavior for the German sites indicates decreasing aerosol scattering and increasing aerosol absorption. This effect may be due to decreasing sulfate and increasing carbonaceous aerosol burden. At noon the modeled and observed 1970s minus 1960s curves agree quite well (red lines in Figure 8). However, the model does not reproduce the negative observational differences shown for high solar zenith angles. The discrepancy

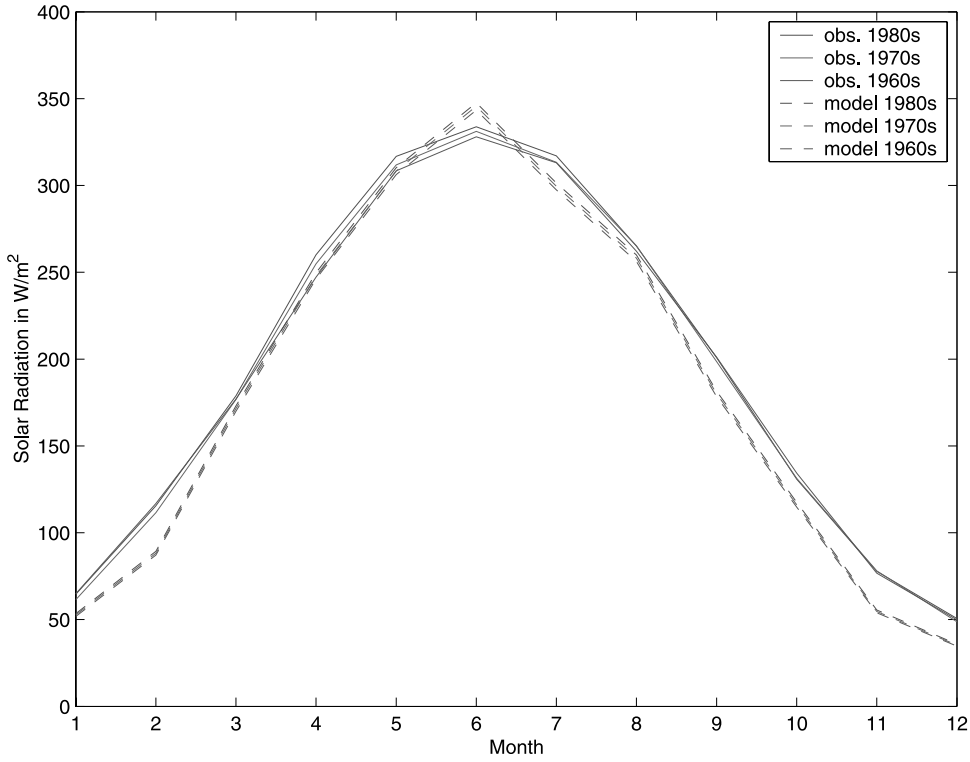

Figure 7. Decadal mean clear-sky global solar radiation at the surface for the German sites. Solid lines are the observations, and dashed lines are the modeled global solar radiation monthly means for the low-BC scenario. See color version of this figure at back of this issue.

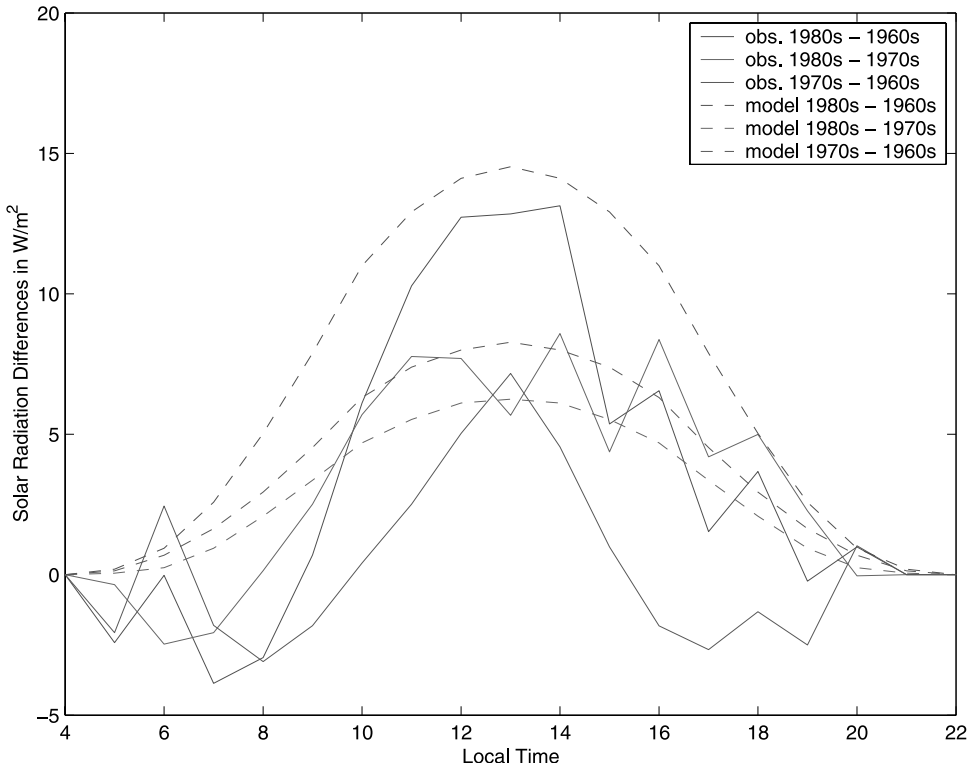

Figure 8. Differences of the decadal mean diurnal cycles of clear-sky global solar radiation at the surface for the German sites. Solid lines are the observations, and dashed lines are the modeled differences for the low-BC scenario. See color version of this figure at back of this issue.

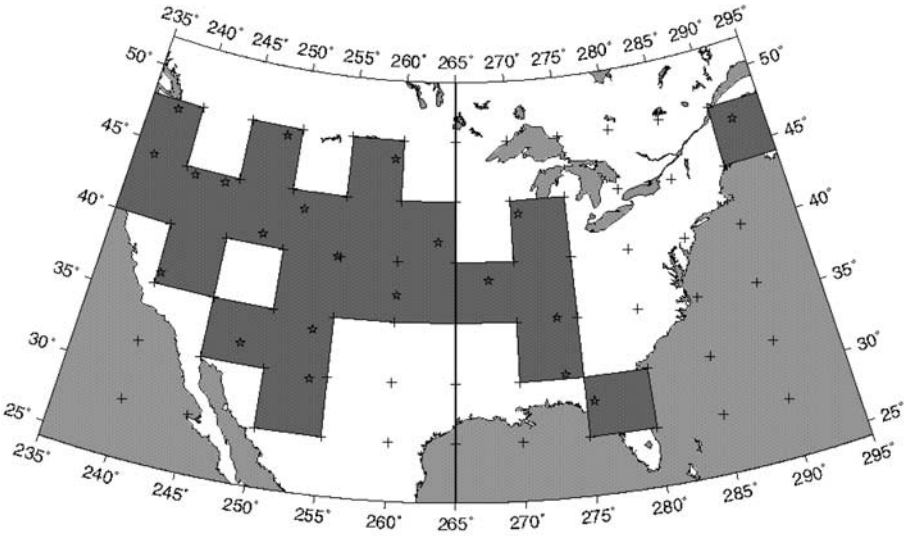

Figure 9. Distribution of the selected diffuse solar radiation grid boxes for the United States. Stars mark the corresponding observational sites. Demarcation line between western and eastern United States is shown.

between model and observation in the diurnal cycle of the solar radiation implies that sulfate concentrations might have been reduced, while carbonaceous aerosol might have increased more effectively than modeled during the 1960s and 1970s. For the consecutive decade in the 1980s the observed changes are mainly positive throughout the day. Model and observation in the 1980s agree quite well for the low BC-scenario as shown in Figure 8 (green curves). Hence the model overestimates the 3-decade difference in solar radiation due only to the first decades.

5. Modeled and Observed Direct/Diffuse Ratio of Solar Radiation

[21] Observations of clear-sky global solar radiation alone cannot provide enough information to retrieve broadband aerosol optical thickness and single-scattering albedo. Yet both parameters are needed to constrain the direct aerosol forcing. However, some information on aerosol scattering and absorption can indirectly be gained with the separate analysis of the direct and diffuse solar radiation. The direct solar radiation B is the energy flux on a horizontal area directly coming from the Sun disk. Diffuse solar radiation D is the energy flux reaching a horizontal area coming from the sky dome. At clear-sky conditions, light is scattered by air molecules (Rayleigh) and aerosols. The direct radiation is obtained by subtracting diffuse radiation from the global solar radiation G. The ratio R of direct to diffuse solar radiation is defined as follows:

$$R = \frac{B}{D} = \frac{G - D}{D}. \quad (1)$$

[22] Declining aerosol scattering over time (e.g., reduced sulfate concentrations) would result in increasing R, while the global solar radiation reaching the ground would stay constant or increase slightly. On the other hand, increasing R and declining global solar radiation indicates higher aerosol absorption (e.g., increased carbonaceous aerosol concentrations) due to the reduction in the diffuse part.

[23] From the mid 1970s on, several stations in the United States and Germany monitored diffuse solar radiation in addition to global solar radiation (see Table 1). In Figure 9 the geographic coordinates of the sites with diffuse radiation recordings are marked as stars. The data are averaged over the time intervals from 1975 to 1985, 1985 to 1990, and the entire time period from 1975 to 1990. Measurements of the diffuse radiation are prone to uncertainties because they rely critically on the correct adjustment of the shadow band. The diffuse radiation can be overestimated if the shadow band does not shield the Sun properly. On the other hand, the shadow band shields not only the Sun disk but also a small fraction of the forward scattered irradiance. The reliability of the measured direct/diffuse ratio is quite uncertain. Hence we focus on the interpretation of the relative differences over time and not on the absolute values.

[24] A parameterization of R originally derived from a statistical meteorological radiation parameterization is used for the model comparison. This parameterization was refined for the NSRDB data by *Maxwell et al.* [1995]. The ratio of broadband direct to diffuse radiation is a function of broadband surface albedo, aerosol optical thickness, and single-scattering albedo in the visible air mass and solar zenith angle. Hourly values of R for every tenth day of the year are computed. The input data are the modeled 5-year means of aerosol optical thickness and single-scattering albedo from 1960 to 1990 for the grid boxes shown in Figure 9, surface albedo from the NSRDB data set, and the aerosol distributions for the low-, modest-, and high-BC scenarios.

6. Results: Direct/Diffuse Ratio

[25] The observed and modeled mean ratios R of the western and eastern United States and German sites are

Table 3. Clear-Sky Direct/Diffuse Solar Radiation Ratio at the Surface for Three Different Model Scenarios and Corresponding Observations

	Model			Observation
	Low BC	Modest BC	High BC	
		Western United States		
1975–1985	7.50	6.89	6.06	6.53
1985–1990	7.26	6.56	5.64	7.04
1975–1990	7.42	6.78	5.92	6.79
1960–1990	7.78	7.20	6.39	
		Eastern United States		
1975–1985	5.25	4.66	3.90	4.60
1985–1990	5.15	4.49	3.66	5.02
1975–1990	5.21	4.61	3.83	4.82
1960–1990	5.55	4.97	4.21	
		Germany		
1975–1985	3.99	2.98	1.99	2.54
1985–1990	4.27	3.24	2.20	2.99
1975–1990	4.08	3.07	2.06	2.76
1960–1990	4.01	2.92	1.89	

listed in Table 3. The observed mean ratios R are 6.79 for the western and 4.82 for the eastern United States. In the east, 1.4 times more solar radiation is scattered in the atmosphere than in the west. However, R for the eastern United States is still (1.7 times) higher than the ratio for Germany. This is not surprising considering the substantially higher aerosol optical thickness in Germany and the lower average altitude of the stations. Noteworthy is the fact that over the 15-year period from 1975 to 1990 all three regions experience a considerable increase in R. The ratio increases are 0.5 and 0.4 for the western and eastern United States, respectively, and 0.5 for Germany. These trends are temporarily simultaneous with the observed weakening of the direct aerosol forcing for Germany (+3 W/m^2) and strengthening for the United States (−7 W/m^2) from the 1970s to the 1980s (compare Table 2).

[26] Figures 10 and 11 show the seasonal cycles of the ratio R for western and eastern United States, respectively. According to *Malm et al.* [1994] the seasonal cycles of sulfate and carbonaceous aerosol depositions were highest in summer and lowest in winter for both regions for the 1988 to 1991 period. Sulfate dominates the aerosol content in the east, whereas organic carbon is the predominant constituent in the west. Therefore the observed direct/diffuse ratio R should be lowest in the months June, July, and August when light-scattering sulfate aerosol reaches the highest concentrations. This is, indeed, the case for the eastern sites as shown in Figure 11. The direct/diffuse ratio in the western part of the United States, however, peaks in summer to fall and declines in the winter months (Figure 10). We suspect that the predominance of carbonaceous aerosols in the west is partly responsible for this cycle. Note that the decline in the ratio R from 1975 to 1990 occurred in fall, winter, and spring in the west and in all months except March and late summer in the east (Figures 10 and 11).

[27] In addition to the observational results the monthly mean modeled direct/diffuse ratios for the modest BC scenarios are also drawn in Figures 10 and 11. The emission

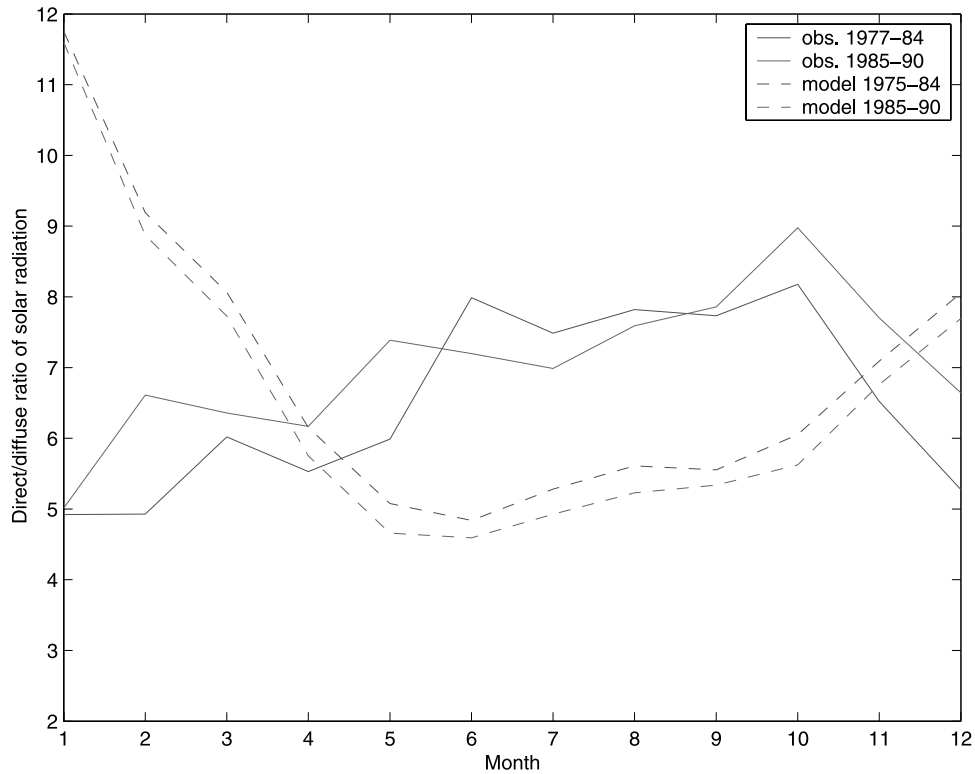

Figure 10. Decadal mean direct/diffuse ratios of clear-sky solar radiation for the western United States. Solid lines are the observations, and dashed lines are the modeled monthly mean ratios for the modest-BC scenario. See color version of this figure at back of this issue.

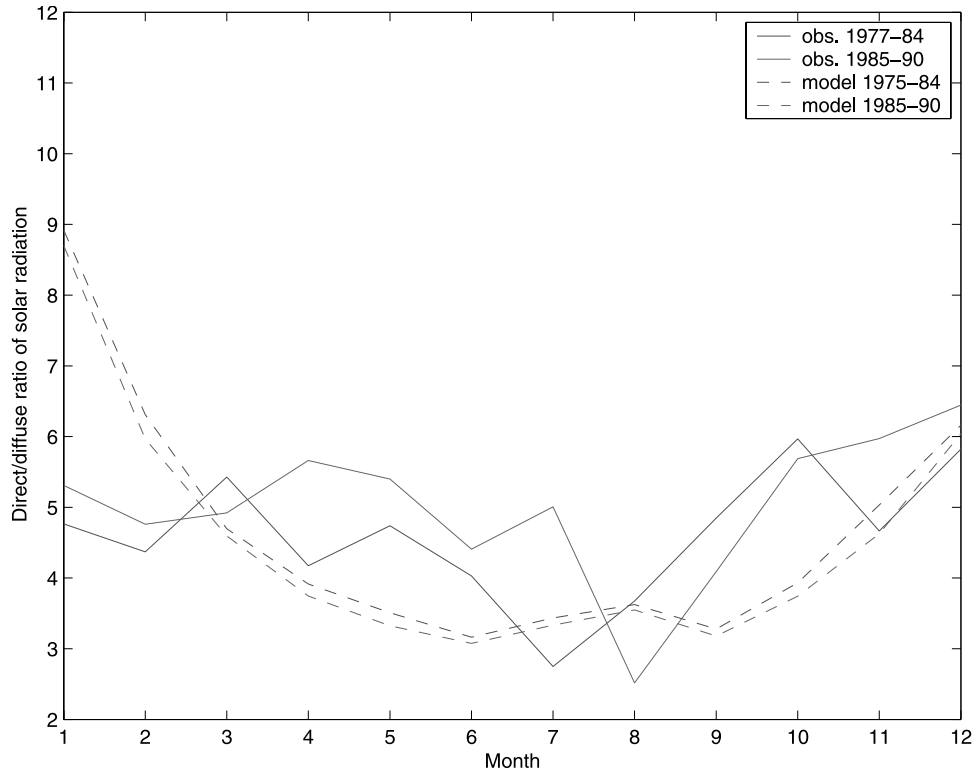

Figure 11. Decadal mean direct/diffuse ratios of clear-sky solar radiation for the eastern United States. Solid lines are the observations, and dashed lines are the modeled monthly mean ratios for the modest-BC scenario. See color version of this figure at back of this issue.

model exaggerates the seasonal cycles of eastern and western United States with a rather high maximum in January for both regions. The difference in the observed seasonality between eastern and western United States is not simulated, which would be offset if the organic carbon concentrations were higher in the west.

[28] However, observed and modeled annual mean values of R agree quite well considering the high uncertainties of both observations and model simulations. The variation between the low- and high-BC scenarios is more prominent for the German sites than for the United States sites. The modest-BC scenario seems to match the observational average in the case of the United States, whereas for the German sites the average observed ratio lies between the modest-BC and high-BC scenario (Table 3).

[29] The modeled sign of the temporal changes of the ratio R is consistent with observations in Germany but differs widely between model and observation for the United States sites. From 1975 to 1990 for the United States the modeled ratio R declines by -3 to -7% depending on the scenario, whereas the observed R increases +9%. We argued in section 4.2 that the aerosol optical thickness in the United States must have increased more substantially in the 1980s than predicted by the model. With the global solar radiation analysis alone, we were not able to draw conclusions about the single-scattering albedo. However, including information of the direct/diffuse ratio, we can further argue that increasing R and declining global solar radiation can only occur if aerosol absorption increases (single-scattering albedo declines). Hence it is assumed that while the modest BC-scenario is a good predictor of the long-term average carbonaceous aerosol burden, the ''temporal changes'' during the period from 1975 to 1990 were more drastic than modeled for the United States (even with the high-BC scenario).

[30] For the German sites, although the sign of the trend in the direct/diffuse ratio is correctly predicted, the observed increase of +18% is underestimated even for the high-BC scenarios. As argued before, with the global solar radiation this may be due to the general overestimation of the sulfate aerosol burden in Germany. Note that the weakening trend in the direct aerosol forcing was correctly predicted (see Table 2). If the sulfate aerosol burden were set generally lower, the high-BC trend from 1975 to 1990 could, indeed, be realistic for Germany according to our findings.

[31] Over a longer time period, recordings of diffuse solar radiation from the year 1964 on are available for two German stations, Hamburg and Hohenpeissenberg. Hamburg is an urban site under maritime influence, and Hohenpeissenberg is located in the rural foothills south of the Alps. Figure 12 shows consecutive 5-year means of the combined record together with the modeled 5-year means for the corresponding two grid boxes. The observed ratio R increases from the mid 1960s on and flattens in the 1970s. It drops in the first half of the 1980s, which conforms to the volcanic eruption of El Chichon in 1982. The ratio increases again and reaches its overall maximum in the second half of the 1980s. The observational data lie well within the modeled range, and the changes over time seem best captured with the modest-BC to high-BC scenario.

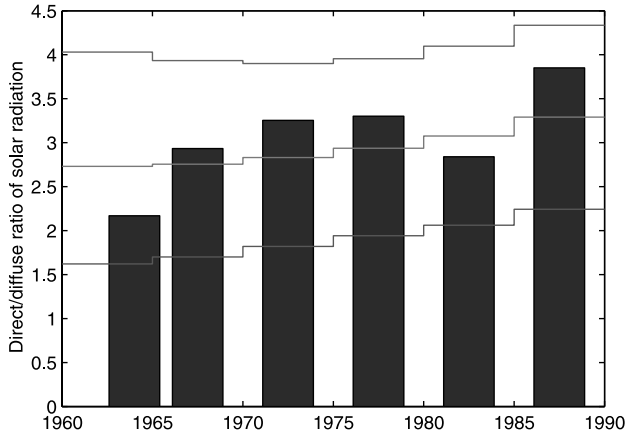

Figure 12. The 5-year mean direct/diffuse ratios of clear-sky solar radiation (1964–1965, 1966–1970, . . .) from two German stations, Hamburg and Hohenpeissenberg, and modeled ratios for corresponding grid boxes for three aerosol scenarios: low BC (upper line), modest BC (middle line), and high BC (lowest line).

[32] In addition to the short time period, Table 3 lists the average modeled direct/diffuse ratio R of the longer 1960–1990 period. In the United States the mean ratio of the longer period is significantly higher for all scenarios than the ratio of the 1975–1990 period. The modeled longer-term ratio R indicates a decline from the 1960s on. This model finding is not in accordance with the observed change in the diurnal cycle of the global solar radiation from the 1960s to the 1970s (Figures 4 and 6). The global radiation increases during midday hours and declines during morning and evening hours from the 1960s to the 1970s. The direct/diffuse ratio is dominated by the midday values and would therefore increase and not decline. For the German sites, however, the 1960–1990 modeled mean direct/diffuse ratio R is lower than the 1975–1990 mean ratio and increased over time in accordance with the observational diurnal cycle shown in Figure 8.

7. Summary

[33] Records of clear-sky global solar radiation at the ground for the western and eastern United States and Germany were analyzed for the 1960s, 1970s, and 1980s. Changes in clear-sky solar radiation are regarded as changes in direct aerosol forcing at the surface. From the 1960s to the 1970s, no trends could be detected either in both parts of the United States or in Germany. Notwithstanding, significant changes in direct aerosol forcing were observed in the 1980s, albeit opposite in sign for the United States and for the German sites. While the aerosol forcing at the surface weakened by +3 W/m^2 in Germany, it strengthened by −8 W/m^2 in the western and −7 W/m^2 in the eastern United States from the 1960s to the 1980s. According to *Malm et al.* [1994], aerosol concentrations are generally higher in the east than in the west of the United States. This result is also reflected in higher mean surface solar radiation in the west. The trends in clear-sky global solar radiation are not uniformly distributed over the day. They show a distinct zenith angle-dependent pattern for all three regions, which points to distinct temporary variations in scattering and absorption of sunlight. This feature can be explained by changing aerosol concentrations of scattering sulfate and absorbing carbonaceous aerosols. The portioning of scattering and absorbing aerosols, namely, the correct prediction of optical thickness and the single-scattering albedo, is the main obstacle for constraining atmospheric net cooling or heating. Measured ratios of direct to diffuse solar radiation were used to assess variations in scattering and absorption of sunlight during the 1975–1990 period. In all three analyzed regions the ratios show an increase of similar magnitude despite the observed opposite trends in solar radiation between the United States and Germany for the same time period. Two German sites reveal the same increasing tendency even for the longer 1960–1990 period. We used a global aerosol model developed by *Tegen et al.* [2000] to verify these observed changes. Modeled aerosol forcing scenarios were calculated for time-dependent emission scenarios of carbonaceous and sulfate aerosols and for other major aerosol components. The modeled changes in surface aerosol forcing, optical thickness, and single-scattering albedo are based on fossil fuel burning usage data from 1960 through 1990. For the western and the eastern parts of the United States the model-derived mean clear-sky global solar radiation is fairly constant throughout the 3 decades, which is not in accordance with the observations. For Germany the observed +3 W/m^2 increase in global solar radiation is well simulated, although it occurs over 3 decades and not the last decade. The model considerably underestimates the long-term mean clear-sky solar radiation that may be due to the observed excessive sulfate burden over Germany [see *Tegen et al.*, 2000]. The modeled direct/diffuse ratios agree quite well with the observations. However, the 15-year modeled trend is opposite in sign in the United States and is too weak in Germany compared to observations.

[34] We suspect that anthropogenic sulfate aerosol concentrations declined during the 1960–1990 period in the United States and in Germany. For Germany this reduction may have been stronger than modeled. For the United States (and Germany in the 1970s), increasing anthropogenic carbonaceous aerosol concentrations must have offset this sulfate effect. The analysis indicates that for the United States, modeled strengthening in carbonaceous aerosol forcing may be underestimated even with the high-BC scenario. In the 1980s the carbonaceous aerosol increase presumably outweighed the sulfate reduction in the United States, whereas in Germany the sulfate reduction dominated. For Germany the low-BC scenario (slight weakening of carbonaceous aerosol forcing) seems to capture the observed increasing trend in surface solar radiation rather well, but with a stronger sulfate reduction, even the modest-BC or high-BC scenario seems realistic.

8. Conclusions

[35] How do these decadal mean climatologies of solar radiation compare to direct aerosol radiative forcings measured in field experiments? During the TARFOX experiment

the measured diurnal mean variability of aerosol-induced solar heating ranged from -5 to -35 W/m^2 at the surface [*Russell et al.*, 1999]. The east coast haze plume is optically thick at this time of the year and can be regarded as an upper limit. *Keil et al.* [2001] investigated aerosol absorption at a rural site in Germany. They measured clear-sky solar forcing at the surface between maritime and polluted air masses ranging from -10 to -17 W/m^2. This seems typical for German sites. Another field example is INDOEX, the experiment over the tropical northern Indian Ocean. During this field campaign, diurnal averaged clear-sky aerosol forcings of -12 to -30 W/m^2 at the surface were measured for the winters of 1998 and 1999. Considering these numbers, the observed climatological mean changes of -8 W/m^2 for the western United States, -7 W/m^2 for the eastern United States, and +3 W/m^2 for Germany from 1960 to 1990 seem within a realistic range.

[36] Other factors besides the aerosol emission rates from which the aerosol forcing scenarios were derived can lead to discrepancies between observed and modeled direct aerosol forcing trends. Inaccurate optical properties (internal versus external mixture) of otherwise correctly represented aerosol distributions may be one factor. However, such an effect would influence both German and U.S. aerosol forcing scenarios in the same way and cannot be responsible for the discrepancies between both regions. Moreover, changes over time in the combustion efficiency would most likely be similar in both regions since both countries share a similar industrial and technological level.

[37] Intercontinental transport of episodic air pollution might also play a larger role than expected. For example, three to five episodic outbreaks of air pollution transported from Asia to North America are observed annually [*Yienger et al.*, 2000], which may not be captured by the model. Since anthropogenic aerosol emission rates (black carbon and sulfate) in China increased drastically in the last decades [*Tegen et al.*, 2000], it might be expected that these increases contribute to the direct aerosol forcing intensification in the western United States. The TARFOX experiment unveiled increasing carbon mass fractions with altitude, suggesting that ground-based measurement (used for validation of modeled aerosol distributions) significantly underestimates column mass concentrations and therefore its importance for aerosol optical thickness and single-scattering albedo [*Novakov et al.*, 1997]. The higher aerosol layers are typically aged layers, which could have been transported from remote regions. While effective filtering of industrial air pollution in the 1980s may have changed the aerosol size distribution and consequently lifetime, aerosol size distributions were fixed in the model. Germany, a major source region of anthropogenic aerosols in western Europe, is now less polluted than it was in the 1960s and than expected by the model, whereas the remote rural sites in the United States tend to be more polluted than before and more polluted than simulated with the emission model. This observation indicates the possible effect of size reduction, longer lifetime, and increasing transport.

[38] Furthermore, observed increases in relative humidity in the last decades [e.g., *Gaffen and Ross*, 1999] could have lead to aerosol particle growth and hence increased aerosol scattering. The model does handle particle growth with increased relative humidity, but long-term changes in relative humidity were not considered.

[39] In general, we postulated that observed changes in clear-sky surface solar radiation are changes in direct aerosol radiative forcing. We cannot totally exclude systematic measurement errors and changes in cloud coverage as possible reasons. However, despite the enormous uncertainties involved in the observational data as well as in the emission scenarios, the combination of both methods provides new information about direct aerosol radiative forcing and justifies this approach.

[40] **Acknowledgments.** We would like to thank the German Weather Service and the National Climate Data Center of NOAA for providing the data sets. We also thank the anonymous reviewers and Dorothy Peteet for their thoughtful suggestions. This work was sponsored by NASA's Global Aerosol Climatology Program grant NAG-7687.

References

Gaffen, D. J., and R. J. Ross, Climatology and trends of U. S. surface humidity and temperature, *J. Clim.*, *12*, 811–828, 1999.

Hansen, J. E., and A. A. Lacis, Sun and dust versus greenhouse gases: An assessment of their relative roles in global climate change, *Nature*, *346*, 713–719, 1990.

Hansen, J. E., M. Sato, R. Ruedy, A. Lacis, and V. Oinas, Global warming in the twenty-first century: An alternative scenario, *Proc. Natl. Acad. Sci. U. S. A.*, *97*, 9875–9880, 2000.

Jacobson, M. Z., Strong radiative heating due to the mixing state of black carbon in atmospheric aerosols, *Nature*, *409*, 695–697, 2001.

Keil, A., M. Wendisch, and E. Brueggemann, Measured profiles of aerosol particle absorption and its influence on clear-sky solar radiative forcing, *J. Geophys. Res.*, *106*(D1), 1237–1247, 2001.

Kiehl, J. T., and B. P. Briegleb, The relative roles of sulfate aerosols and greenhouse gases in climate forcing, *Science*, *260*, 311–314, 1993.

Koch, D., D. Jacob, I. Tegen, D. Rind, and M. Chin, Tropospheric sulfur simulation and sulfate direct radiative forcing in the Goddard Institute for Space Studies General Circulation Model, *J. Geophys. Res.*, *104*(D23), 23,799–23,822, 1999.

Lavanchy, V., H. W. Gaeggeler, U. Schotterer, M. Schwinkowski, and U. Baltensperger, Historical record of carbonaceous particle concentrations from European high-alpine glacier (Colle Gnifetti, Switzerland), *J. Geophys. Res.*, *104*, 21,227–21,237, 1999.

Lefohn, A. S., J. D. Husar, and R. B. Husar, Estimating historical anthropogenic global sulfur emission patterns for the period 1850–1990, *Atmos. Environ.*, *33*, 3435–3444, 1999.

Liepert, B. G., Recent changes in solar radiation under cloudy conditions in Germany, *Int. J. Climatol.*, *17*, 1581–1593, 1997.

Liepert, B. G., and G. J. Kukla, Decline in global solar radiation with increased horizontal visibility in Germany between 1964 and 1990, *J. Clim.*, *10*, 2391–2401, 1997.

Liepert, B. G., and U. Lohmann, A comparison of surface observations and ECHAM4-GCM experiments and its relevance to the indirect aerosol effect, *J. Clim.*, *14*, 1078–1091, 2001.

Malm, W. C., J. F. Sisler, D. Huffman, R. A. Eldred, and T. A. Cahill, Spatial and seasonal trends in particle concentration and optical extinction in the United States, *J. Geophys. Res.*, *99*(D1), 1347–1370, 1994.

Maxwell, E. L., W. F. Marion, D. R. Myers, M. D. Rymes, S. M. Wilcox, *Final Technical Report Volume 2: National Solar Radiation Database (1961–1990)*, Natl. Renewable Energy Lab., Golden, Colo., 1995.

Myhre, G., F. Stordal, K. Restad, and I. S. A. Isaksen, Estimation of the direct radiative forcing due to sulfate and soot aerosols, *Tellus, Ser. B*, *50*, 463–477, 1998.

Novakov, T., D. A. Hegg, and P. V. Hobbs, Airborne measurements of carbonaceous aerosols on the East Coast of the United States, *J. Geophys. Res.*, *102*(D25), 30,023–30,030, 1997.

Penner, J. E., C. C. Chuang, and K. Grant, Climate forcing by carbonaceous and sulfate aerosols, *Clim. Dyn.*, *14*, 839–851, 1998.

Russell, P. B., J. M. Livingston, P. Hignett, S. Kinne, J. Wong, A. Chien, R. Bergstrom, P. Durkee, and P. V. Hobbs, Aerosol-induced radiative flux changes off the United States mid-Atlantic coast: Comparison of values calculated from sunphotometer and in situ data with those measured by airborne pyranometer, *J. Geophys. Res.*, *104*(D2), 2289–2307, 1999.

Satheesh, S. K., and V. Ramanathan, Large differences in tropical aerosol forcing at the top of the atmosphere and Earth's surface, *Nature*, *405*, 60–63, 2001.

Schult, I., J. Feichter, and W. F. Cooke, Effect of black carbon and sulfate aerosols on the Global Radiation Budget, *J. Geophys. Res.*, *102*(D25), 30,107–30,117, 1997.

Tegen, I., D. Koch, A. A. Lacis, and M. Sato, Trends in tropospheric aerosol loads and corresponding impact on direct radiative forcing between 1950 and 1990: A model study, *J. Geophys. Res.*, *105*(D22), 26,971–26,989, 2000.

Yienger, J. J., M. Galanter, T. A. Holloway, M. J. Phadnis, S. K. Guttikunda, G. R. Carmichael, W. J. Moxim, and H. Levy, II, The episodic nature of air pollution transport from Asia to North America, *J. Geophys. Res.*, *105*(D22), 26,931–26,945, 2000.

B. Liepert, Lamont-Doherty Earth Observatory, P.O. Box 1000, Palisades, NY 10964, USA. (liepert@ldeo.columbia.edu)

I. Tegen, Max Planck Institute for Biogeochemistry, Carl-Zeiss-Promenade 10, D-07745 Jena, Germany. (itegen@bgc.-jena.mpg.de)

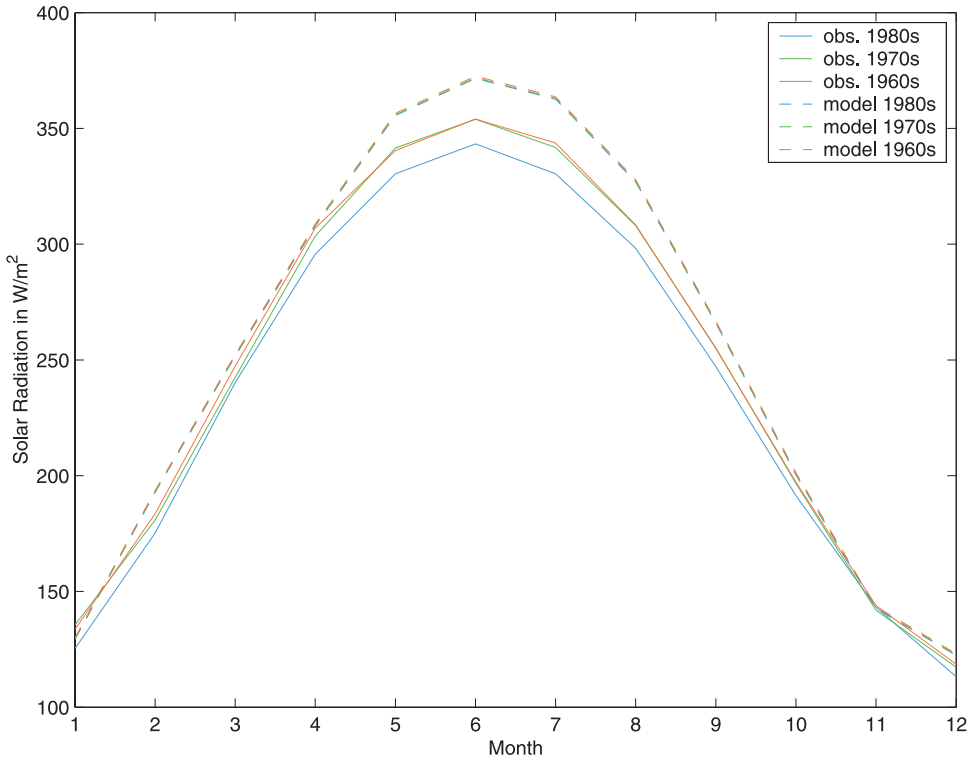

Figure 3. Decadal mean clear-sky global solar radiation at the surface for the western United States. Solid lines are the observations, and dashed lines are the modeled solar radiation monthly means for the high–black carbon (BC) scenario.

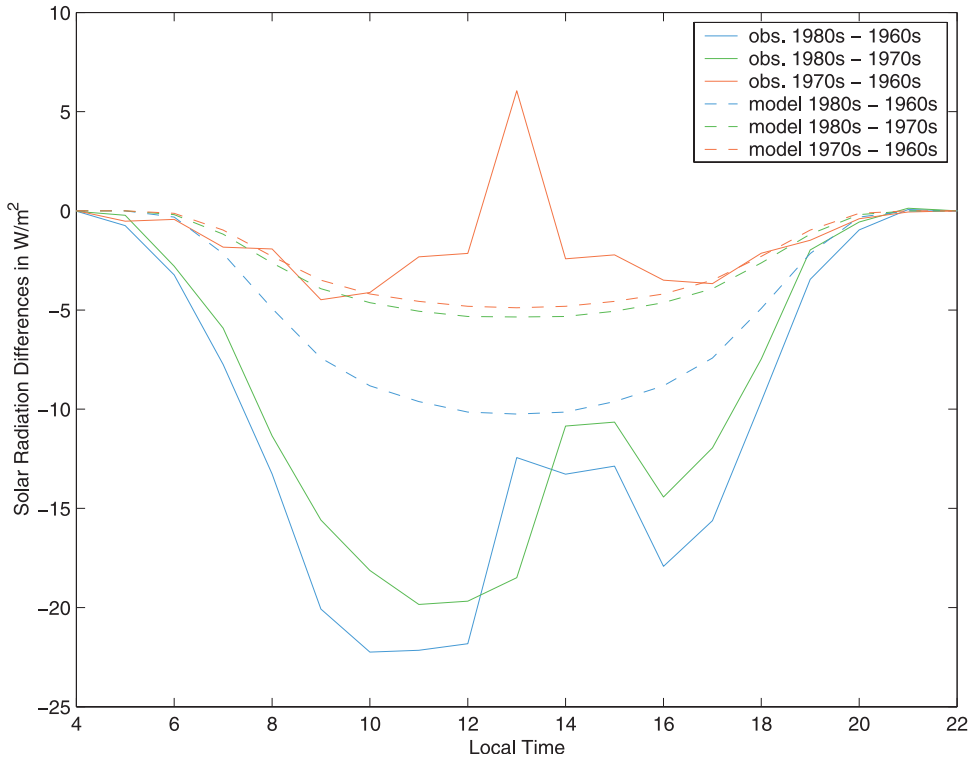

Figure 4. Differences in decadal mean diurnal cycles of clear-sky global solar radiation at the surface for the western United States. Solid lines are the observations, and dashed lines are the modeled differences for the high-BC scenario.

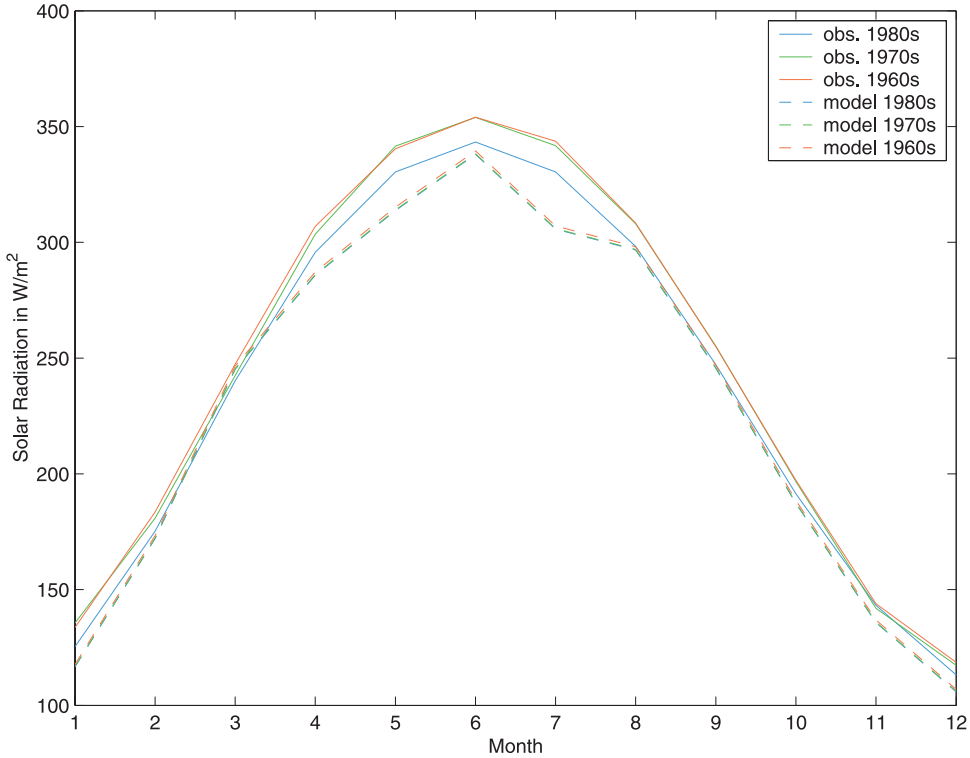

Figure 5. Decadal mean clear-sky global solar radiation at the surface for the eastern United States. Solid lines are the observations, and dashed lines are the modeled solar radiation monthly means for the high-BC scenario.

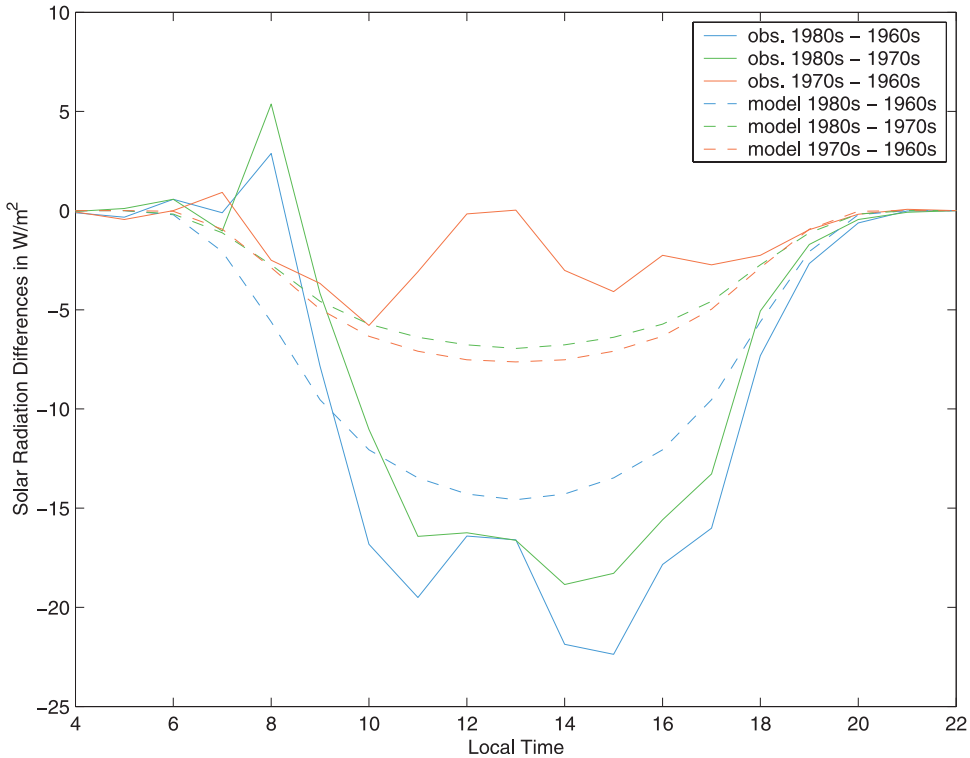

Figure 6. Differences in decadal mean diurnal cycles of clear-sky global solar radiation at the surface for the eastern United States. Solid lines are the observations, and dashed lines are the modeled differences for the high-BC scenario.

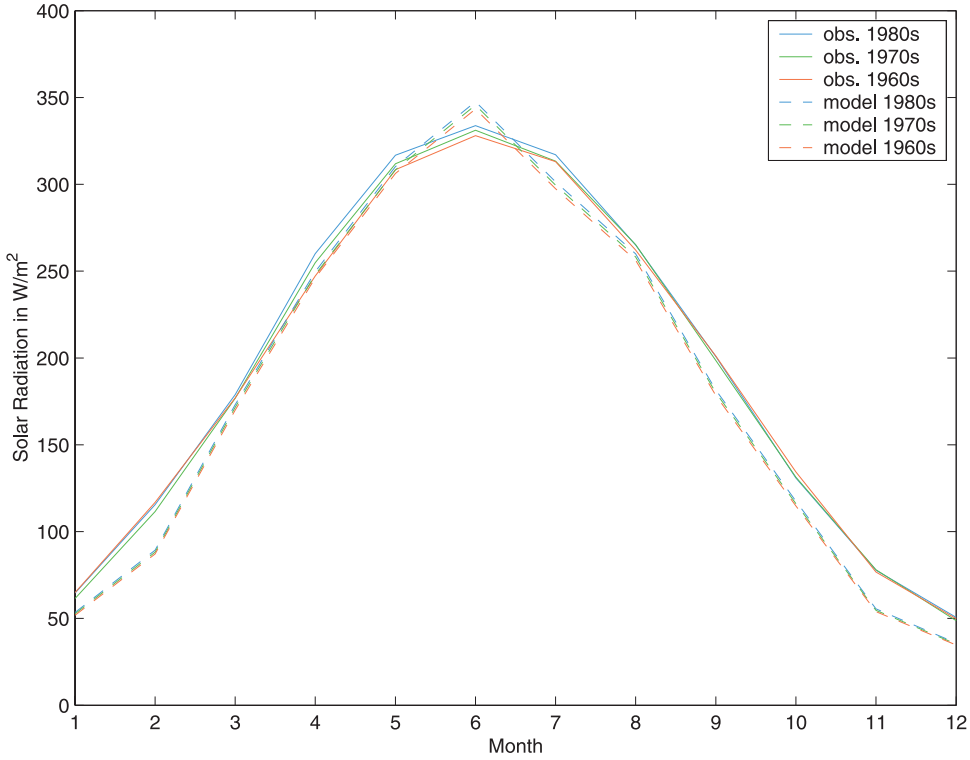

Figure 7. Decadal mean clear-sky global solar radiation at the surface for the German sites. Solid lines are the observations, and dashed lines are the modeled global solar radiation monthly means for the low-BC scenario.

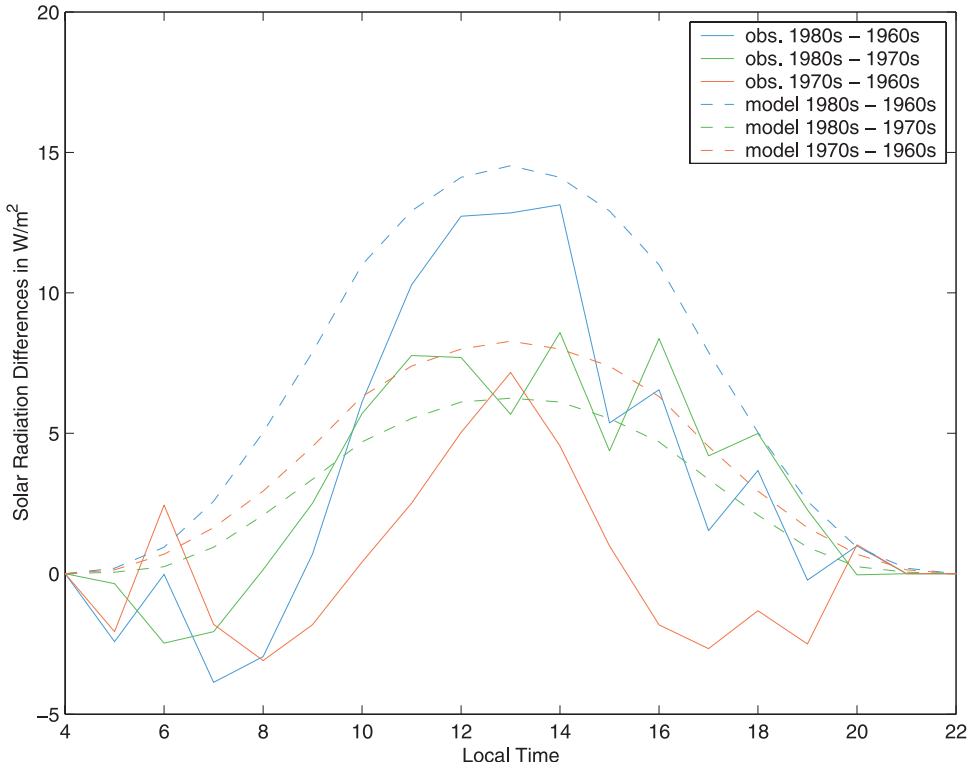

Figure 8. Differences of the decadal mean diurnal cycles of clear-sky global solar radiation at the surface for the German sites. Solid lines are the observations, and dashed lines are the modeled differences for the low-BC scenario.

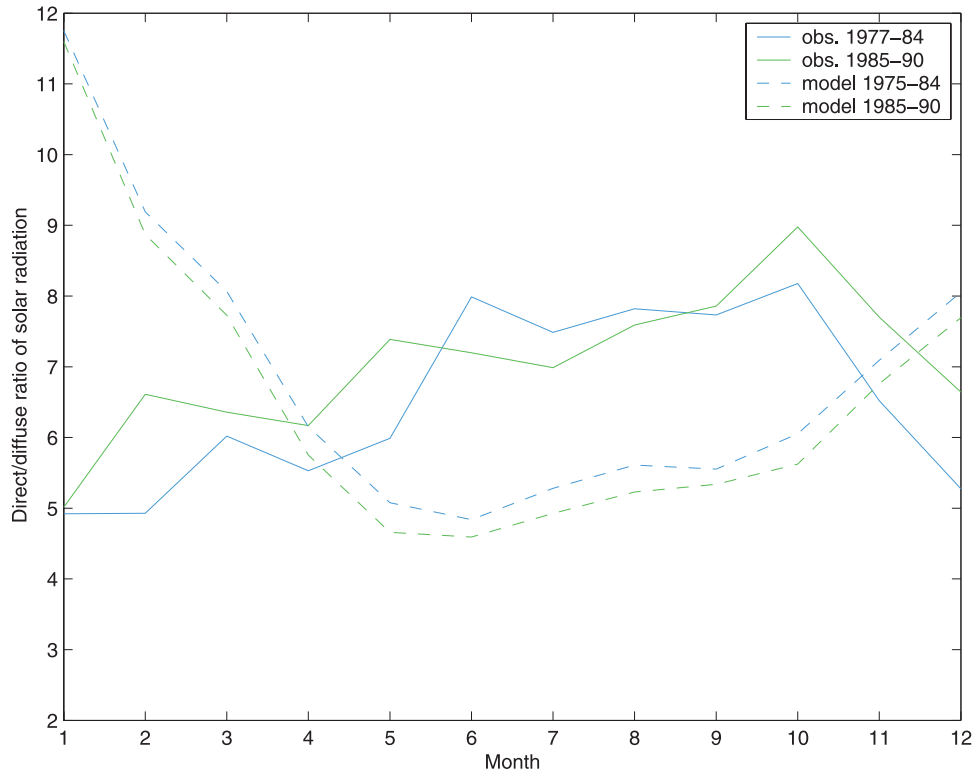

Figure 10. Decadal mean direct/diffuse ratios of clear-sky solar radiation for the western United States. Solid lines are the observations, and dashed lines are the modeled monthly mean ratios for the modest-BC scenario.

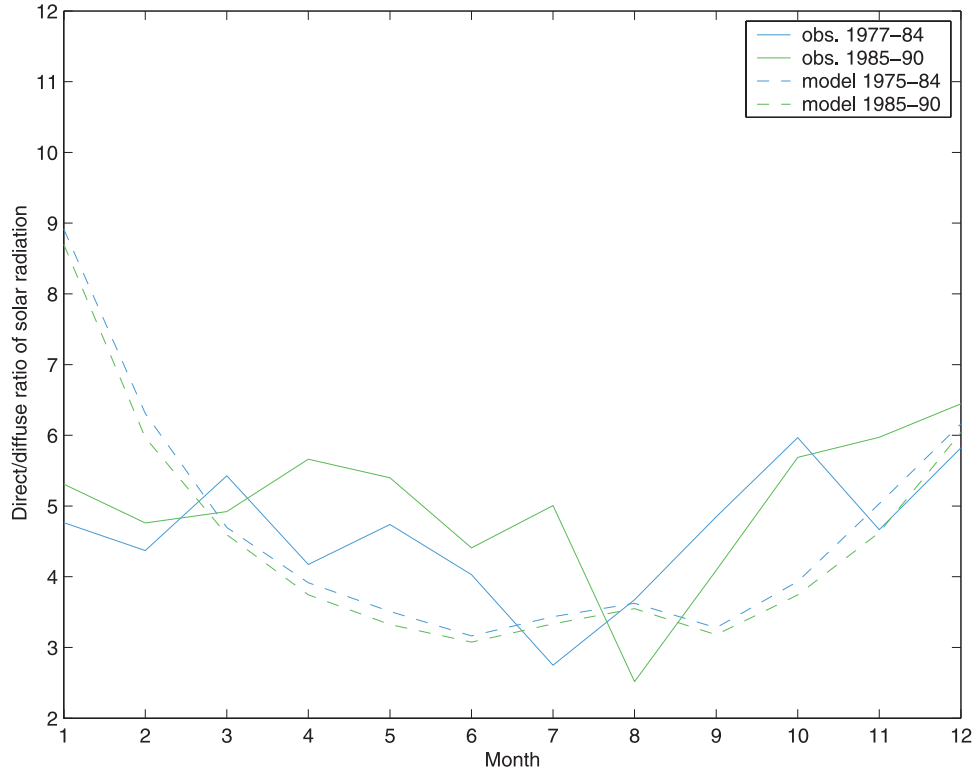

Figure 11. Decadal mean direct/diffuse ratios of clear-sky solar radiation for the eastern United States. Solid lines are the observations, and dashed lines are the modeled monthly mean ratios for the modest-BC scenario.